



MECHANICAL BEHAVIOR AND SHEAR STRENGTH EVALUATION OF DISK SHEAR-KEY UNDER TENSILE FORCE AND SHEAR FORCE

Y. Ishida⁽¹⁾, H. Sakata⁽²⁾, Y. Takase⁽³⁾, Y. Maida⁽⁴⁾, T. Sato⁽⁵⁾, M. Kubota⁽⁶⁾

⁽¹⁾ Graduate Student, Dept. of Arch. and Build. Eng., Tokyo Tech, M. Eng., ishida.y.ah@m.titech.ac.jp
JSPS Research Fellow DC

⁽²⁾ Professor, Dept. of Arch. and Build. Eng., Tokyo Tech, Dr. Eng., sakata.h.aa@m.titech.ac.jp

⁽³⁾ Associate Professor, College of Design and Manufacturing Tech., Muroran Tech, Dr. Eng., y.takase@mmm.muroran-it.ac.jp

⁽⁴⁾ Senior Researcher, National Institute for Land and Infrastructure Management, Dr. Eng., maida-y92gy@mlit.go.jp

⁽⁵⁾ TOBISHIMA Corporation, Takumi_Satou@tobishima.co.jp

⁽⁶⁾ TOBISHIMA Corporation, Masaharu_Kubota@tobishima.co.jp

...

Abstract

The external seismic retrofitting is one of the seismic retrofitting methods for existing reinforced concrete buildings. The demand for external seismic retrofitting is increasing because it can be constructed while the building is still functional. The sufficient shear strength and high stiffness are required for the joint of seismic retrofitting. Furthermore, since the existing frame and the reinforcing frame are eccentric, in addition to the shear force, the compressive force and the tensile force due to the eccentric bending moment act on the joint, and the combined stress appears at the joint of external seismic retrofitting.

The disk shear-key is a composite shear resistance system composed of a steel disk and an anchor bolt. The disk shear-key has high stiffness and shear strength as compared with the general post-installed anchor. In the previous study, it is suggested that the expected shear strength cannot be demonstrate when tensile force acts on the disk shear-key. Therefore, in the current design and construction method, it is assumed that the disk shear-keys are placed in the center of the span and bear only shear force. Moreover, for the tensile force due to the eccentric moment, the post-installed anchors are placed at both ends of the span and bear the tensile force. In order to make effective use of the disk shear-key, it is necessary to grasp the mechanical behavior under combined stress and arrange it efficiently.

In this study, in order to investigate the mechanical behavior of the disk shear-key under combined stress of shear force and tensile force, specimens of the retrofitting joint composed of the existing concrete, one disk shear-key and the retrofitting concrete were prepared and tested by applying a cyclic shear force while applying a constant tensile force. A total of eight specimens were prepared with various parameters, which are the diameter of the steel disk R_d , the embedded length of the anchor bolt l_e , and the tensile force ratio η' . Here, the tensile force ratio is the ratio of the tensile axial force to the tensile strength of the disk shear-key.

The shear strength of the specimens in this experiment was less than the ultimate shear strength according to the current evaluation formula, and it decreased as the tensile force increased. However, when the vertical stress generated at the joint surface is zero, the shear strength of the disk shear-key can be roughly estimated by the design shear strength according to the current design evaluation formula. The relative vertical displacement also increase as the tensile force is applied. Furthermore, in the case of application to the external seismic retrofitting, the relative vertical displacement increases even when tensile force is not applied. It is suggested that the steel disk slips out, and it is believed that the shear resistance decreases due to the strength reduction in the bearing stress area of the concrete.

Therefore, the evaluation formula was modified in consideration of the slipping out of the steel disk and the reduction of restraint effect by anchor bolt due to the tensile force. It was evaluated almost accurately with the experimental results.

Keywords: Shear-key; Combined stress; Shear strength; Joint element; External seismic retrofitting



1. Introduction

The external seismic retrofitting shown in Fig.1, is one of the seismic retrofitting methods for existing reinforced concrete buildings. The demand for external seismic retrofitting is increasing because it can be constructed while the building is still functional. The sufficient shear strength and high stiffness are required for the joint of seismic retrofitting. Furthermore, since the existing frame and the retrofitting frame are eccentric, in addition to the shear force, the compressive force and the tensile force due to the eccentric bending moment act on the joint, and the combined stress appears at the joint of external seismic retrofitting.

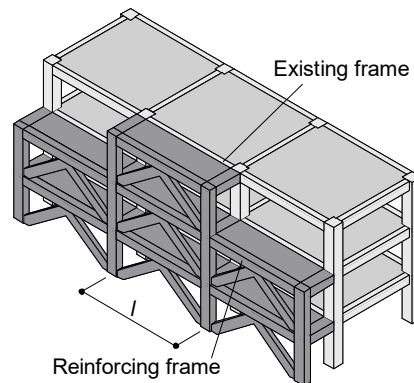
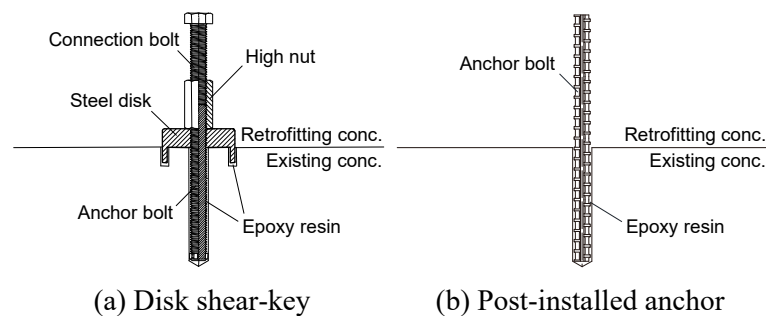


Fig. 1 – Outline of external seismic retrofitting

The disk shear-key shown in Fig.2(a), is a composite shear resistance system composed of a steel disk and an anchor bolt. The disk shear-key has high stiffness and shear strength as compared with the general post-installed anchor shown in Fig.2(b).



(a) Disk shear-key

(b) Post-installed anchor

Fig. 2 – Type of joint element

In the previous study, the fundamental performance of the disk shear-key was grasped by reference [1]. Furthermore, the experiments applied to internal seismic retrofitting^[2] and the experiments applied to external seismic retrofitting^[3] were also conducted. Among them, it is suggested that the expected shear strength cannot be demonstrate when tensile force acts on the disk shear-key. Therefore, in the current design and construction method according to reference [4], it is assumed that the disk shear- keys are placed in the center of the span, as shown in Fig.3. Here, the average shear force is subjected the disk shear-key, however the disk shear-key cannot resist the tensile force. For the tensile force due to the eccentric moment, the post-installed anchors are placed at both ends of the span and bear the tensile force.

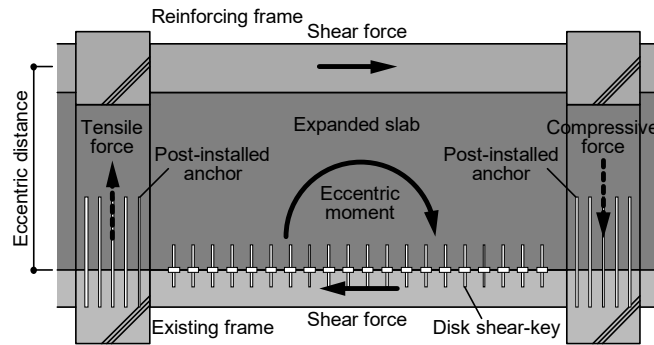


Fig. 3 – Design concept of joint using disk shear-key

In order to make effective use of the disk shear-key, it is necessary to grasp the mechanical behavior under combined stress and arrange it efficiently. Therefore, in this study, the disk shear-key was tested under cyclic shear force along with constant tensile force.

2. Outline of experiment

2.1 Details of specimens

The details of the specimens are shown in Fig.4. The specimen composed of the existing concrete, one disk shear-key and the retrofitting concrete. First, the concrete on the existing side was cast, and after demolding, a hole for installing a disk shear-key was drilled using a wet core drill. After sufficient drying, an adhesive of epoxy resin was injected and a disk shear-key was installed. Next, reinforcement rebars and a steel plate which welded headed studs were installed, and the concrete on the reinforcing side was cast. A hole was provided in the center of the steel plate so that the tensile force could be applied directly to the disk shear-key through the anchor bolt. Here, it is assumed that the actual joint surface resists the tensile force due to the vertical stress caused by the adhesion of the joint surface. However, in this experiment, in order to understand the pure mechanical behavior of the disk shear-key under a constant tensile force, the grease was applied to the joint of specimens.

For the specimens in this experiment, there are full-scale series ($\phi 90$ series) and 1/2-scale series ($\phi 45$ series). For the $\phi 90$ series, the diameter of the steel disk R_d is 90mm and the diameter of the anchor bolt d_a is 20mm. On the other hand, for the $\phi 45$ series, R_d is 45mm and d_a is 10mm. In addition, the embedded depth of the steel disk h_d is 19mm for the $\phi 90$ series and 9.5mm for the $\phi 45$ series. Moreover, the thickness of cover concrete is 30mm for the $\phi 90$ series and 15mm for the $\phi 45$ series.

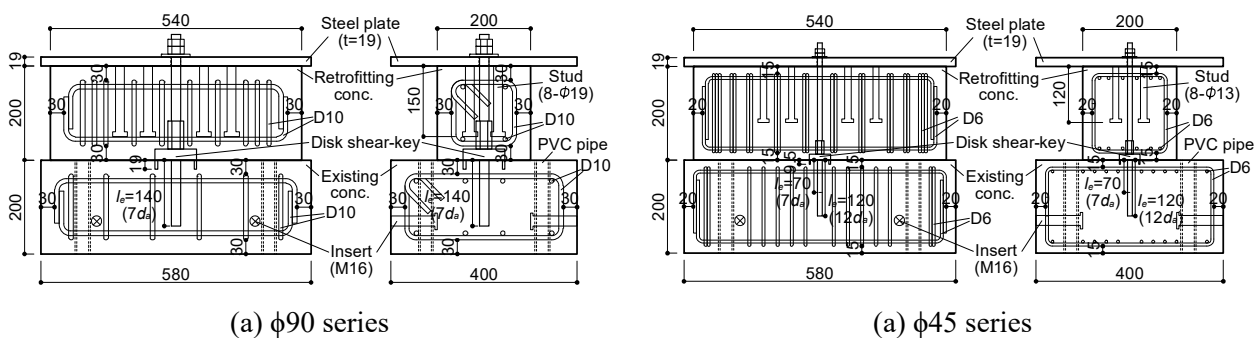


Fig. 4 – Details of specimens (unit : [mm])



2.2 Parameters of specimen

The parameters of specimen are indicated in Table 1, the material properties of concrete are indicated in Table 2, and the material properties of steel are indicated in Table 3. The eight specimens were prepared with various parameters, which are the diameter of the steel disk R_d , the embedded length of the anchor bolt l_e , and the tensile force ratio η' . In addition, the design strength of concrete is common to all specimens, and the existing side is $F_c=21$ and the retrofitting side is $F_c=36$. Here, the tensile force ratio η' is the ratio of the tensile axial force to the tensile strength of the disk shear-key.

Table 1 – Parameters of specimen

Specimen	R_d [mm]	d_a [mm]	l_e [mm]	η' [-]	T_1 [kN]	T_2 [kN]	T_3 [kN]	T_{min} [kN]	T_η [kN]
$\phi 90$ -7da-0	90	20 (M20)	140 (7 d_a)	0	89.3	119.6	63.1	63.1	0
$\phi 90$ -7da-0.25				0.25					15.8
$\phi 90$ -7da-0.5				0.5					31.6
$\phi 45$ -7da-0	45	10 (M10)	70 (7 d_a)	0	18.3	28.4	17.5	17.5	0
$\phi 45$ -7da-0.25				0.25					4.4
$\phi 45$ -7da-0.5				0.5					8.7
$\phi 45$ -12da-0			120 (12 d_a)	0		79.0	30.0	18.3	0
$\phi 45$ -12da-0.5				0.5					9.1

R_d : Diameter of steel disk, d_a : Diameter of anchor bolt, l_e : Embedded length of anchor bolt, η' : Tensile force ratio, T_1 : Yield strength of anchor bolt, T_2 : Cone-type failure strength of concrete, T_3 : Adhesion failure strength of anchor bolt, T_{min} : Tensile strength of disk shear-key, T_η : Applied tensile strength

Table 2 – Material properties of concrete

Series	Existing side					Retrofitting side				
	F_c [N/mm ²]	σ_B [N/mm ²]	ε_c [μ]	E_c [N/mm ²]	σ_t [N/mm ²]	F_c' [N/mm ²]	σ_B' [N/mm ²]	ε_c' [μ]	E_c' [N/mm ²]	σ_t' [N/mm ²]
$\phi 90$ series	21	30.1	2,240	26,800	2.19	36	43.8	2,170	34,900	3.58
$\phi 45$ series		27.1	1,990	27,900	2.21		46.4	2,250	34,500	3.82

F_c, F_c' : Design strength, σ_B, σ_B' : Compressive strength, $\varepsilon_c, \varepsilon_c'$: Strain at compressive strength, E_c, E_c' : Young's modulus, σ_t, σ_t' : Tensile strength

Table 3 – Material properties of steel

Type of steel	σ_y [N/mm ²]	σ_u [N/mm ²]	ε_y [μ]	E_s [N/mm ²]	EL [%]
M20 (for $\phi 90$ series)	392	558	3,990	201,000	15.3
M10 (for $\phi 45$ series)	336	524	3,850	184,000	14.9
D10 (for $\phi 90$ series)	368	527	2,360	201,000	27.7
D6 (for $\phi 45$ series)	299	421	3,830	171,000	15.7

σ_y : Yield strength, σ_u : Ultimate strength, ε_y : Strain at yield strength, E_s : Young's modulus, EL : Elongation after fracture



The tensile strength of the disk shear-key T_{min} is the minimum value of T_1 , T_2 and T_3 obtained according to the reference [5], as shown in Eq. (1)-(8). Further, the applied tensile force T_η was determined by multiplying T_{min} by η' .

[Tensile strength of disk shear-key T_{min}]

$$T_{min} = \min(T_1, T_2, T_3) \quad (1)$$

[Yield strength of anchor bolt T_1]

$$T_1 = \sigma_y \cdot s_c a \quad (2)$$

[Cone-type failure strength of concrete T_2]

$$T_2 = c \sigma_t \cdot A_c \quad (3)$$

$$c \sigma_t = 0.31 \sqrt{\sigma_B} \quad (4)$$

$$A_c = \pi \cdot l_{ce} (l_{ce} + D) \quad (5)$$

[Adhesion failure strength of anchor bolt T_3]

$$T_3 = \tau_a \cdot \pi \cdot d_a \cdot l_{ce} \quad (6)$$

$$\tau_a = \alpha \cdot \tau_{bavg} \quad (7)$$

$$\alpha = 0.5 \left(\frac{c}{l_e} \right) + 0.5 \quad (c/l_e \leq 1), (l_e \leq 10d_a) \quad (8)$$

where σ_y is the yield strength of the anchor bolt [N/mm²]; $s_c a$ is the cross-sectional area of the anchor bolt [mm²]; $c \sigma_t$ is the tensile strength of concrete against cone-type failure [N/mm²]; σ_B is the compressive strength of concrete [N/mm²]; A_c is the effective horizontal projection area of cone-type fracture surface [mm²]; l_{ce} is the embedded length (= l_e) [mm] for calculating the strength of the anchor bolt; D is the diameter of anchor bolt head [mm]; τ_a is the adhesion strength of the adhesive anchor bolt [N/mm²]; τ_{bavg} is the average adhesion strength of the adhesive anchor bolt (= $7\sqrt{\sigma_B/21}$) [N/mm²]; α is the reduction coefficient of adhesion strength due to the edge; c is the edge [mm].

In the specimens of this experiment, the tensile strength T_{min} is determined by the adhesion failure strength T_3 in the series of $l_e=7d_a$. On the other hand, the series of $l_e=12d_a$ is determined by the yield strength of the anchor bolt T_1 . That is, the specimens were designed so that the assumed tensile failure mode differs depending on the embedding length l_e .

2.3 Lading plan

The loading setup is shown in Fig.5. Hydraulic jacks were attached horizontally to left and right at the same height as the joint surface, by which the cyclic shear force was applied. In addition, a center hole jack was attached in the vertical direction. The weight of the loading beam and so on was offsetted, and the predetermined tensile force was applied.

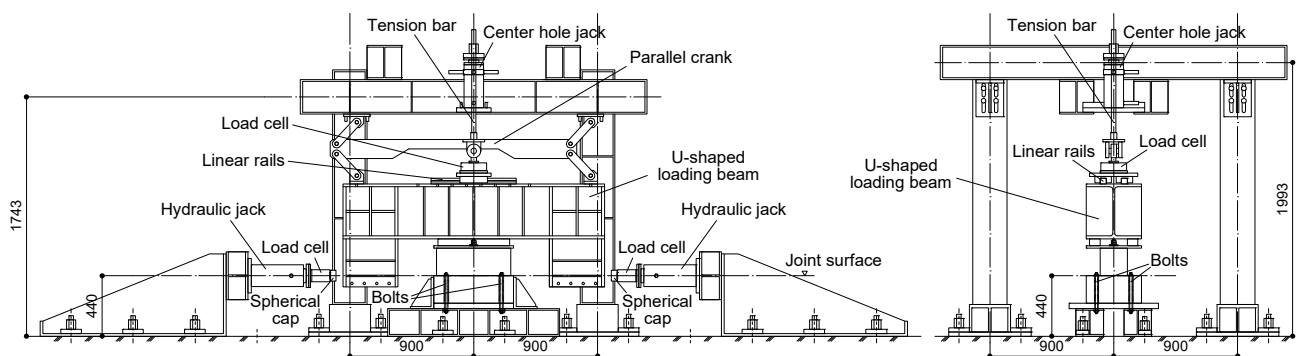


Fig. 5 – Loading setup (unit : [mm])



The loading was controlled by relative horizontal displacement δ_h of the existing concrete and the retrofitting concrete, and was carried out in the cycle shown in Fig.6.

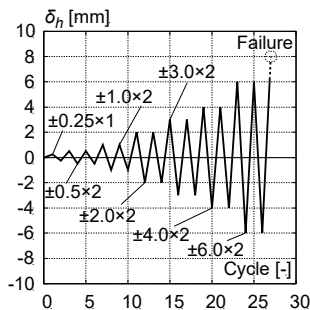


Fig. 6 – Loading cycle

2.4 Measurement plan

The mounting position of the displacement gauge is shown in Fig.7. The relative horizontal displacement and relative vertical displacement of the existing concrete and the retrofitting concrete were measured at two points, and their average values were taken as δ_h and δ_v .

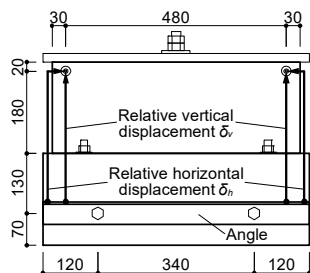


Fig. 7 – Mounting position of displacement gauge (unit : [mm])

The sticking position of the strain gauge is shown in Fig.8. The anchor bolt was machined on both sides from the top to the bottom. The strain gauges were stuck on both sides at $2d_a$, $4d_a$ and $6d_a$ on the existing side and $5d_a$ and $7d_a$ on the retrofitting side from the joint surface.

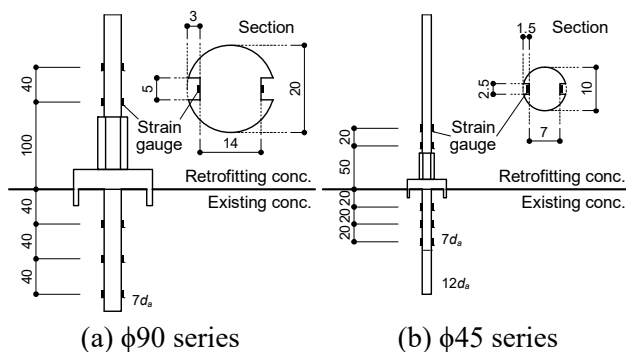


Fig. 8 – Sticking position of strain gauge (unit [mm])

3. Experiment results

3.1 Shear force vs. relative horizontal displacement

The relationship between the shear force Q and the relative horizontal displacement δ_h is shown in Fig.9. Fig.9 also shows the design shear strength Q_{jd} calculated by the current design shear strength evaluation formula^[2] described in Chapter 4. Further, the dots in Fig.9 indicate points at the maximum shear strength Q_{exp} on each of the positive side and the negative side. Here, since the specimen $\phi90-7da-0$ was pre-loaded before conducting



the experiment, the shear strength on the positive side was smaller than the negative side. Therefore, $\phi 90-7da-0$ is mainly described for the maximum shear strength on the negative side.

Focusing on the maximum shear strength Q_{exp} of the three specimens $\phi 90-7da-0$, $\phi 45-7da-0$ and $\phi 45-12da-0$ without tensile force ($\eta'=0$) are approximately equal to the design shear strength Q_{jd} . On the other hand, the five specimens $\phi 90-7da-0.25$, $\phi 90-7da-0.5$, $\phi 45-7da-0.25$, $\phi 45-7da-0.5$, and $\phi 45-12da-0.5$, which were applied to tensile force ($\eta'=0.25, 0.5$), are smaller than Q_{jd} .

When comparing $\phi 45-7da-0$ with $\phi 45-12da-0$ and $\phi 45-7da-0.5$ with $\phi 45-12da-0.5$, in the specimens with embedded length $l_e=7d_a$, the maximum shear strength on the negative side is smaller than the positive side. On the other hand, in the specimens with embedded length $l_e=12d_a$, no significant difference of the maximum shear strength was found between the positive side and negative side, and it showed almost the same behavior.

When focusing on Fig.9(d), (h) and (k), and comparing the envelope curves of each specimen series, it can be seen that the shear strength and stiffness decrease as the tensile force increases. However, in the range of $\eta'=0$ to 0.5 conducted in this experiment, the relative horizontal displacement at maximum shear strength $\delta_h|_{Q_{exp}}$ is within 2mm. This is within the allowable value of the external seismic retrofitting joint [4].

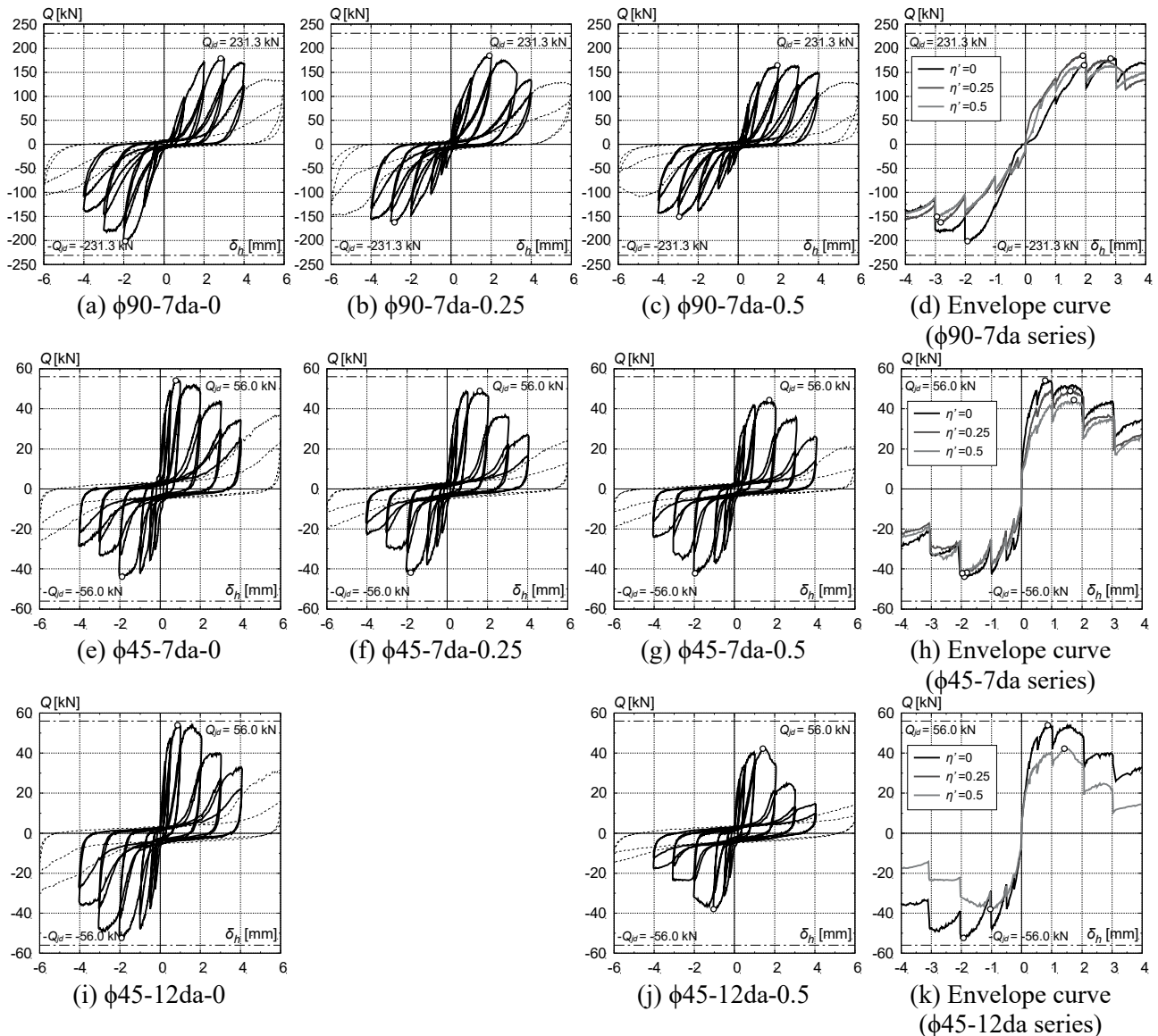
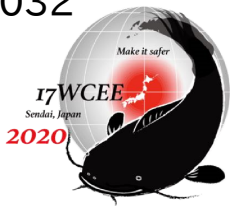


Fig. 9 – Shear force vs. relative horizontal displacement



3.2 Relative vertical displacement vs. relative horizontal displacement

The relationship between relative vertical displacement δ_v and relative horizontal displacement δ_h is shown in Fig.10. The dots indicate the points at the maximum shear strength Q_{exp} for the positive side and the negative side same as Fig.9.

According to the result of the experiment of internal seismic retrofitting^[2], it is shown that relative vertical displacement δ_v is 1/2 of relative horizontal displacement δ_h ($\delta_v=0.5\delta_h$). However, focusing on the three specimens $\phi90-7da-0$, $\phi45-7da-0$, and $\phi45-12da-0$ with $\eta'=0$, the relative vertical displacement δ_v at maximum shear strength Q_{exp} tends to be larger than $\delta_v=0.5\delta_h$. In other words, if the post-installed anchors for tensile force burden are not placed when applying the disk shear-key to external seismic retrofitting, the steel disk will slip out even if no tensile force is generated, compared to when applying to internal seismic retrofitting. As a result, it is thought that the shear strength decreases as the bearing resistance of the concrete decreases.

Next, for the specimens $\phi90-7da-0.25$ and $\phi45-7da-0.25$, the relative vertical displacement δ_v tends to increase with the relative horizontal displacement δ_h at a correlation about $\delta_v=0.75\delta_h$. Furthermore, in the cases of $\phi90-7da-0.5$ and $\phi45-7da-0.5$, the correlation is about $\delta_v=\delta_h$. However, the relative vertical displacement δ_v ,

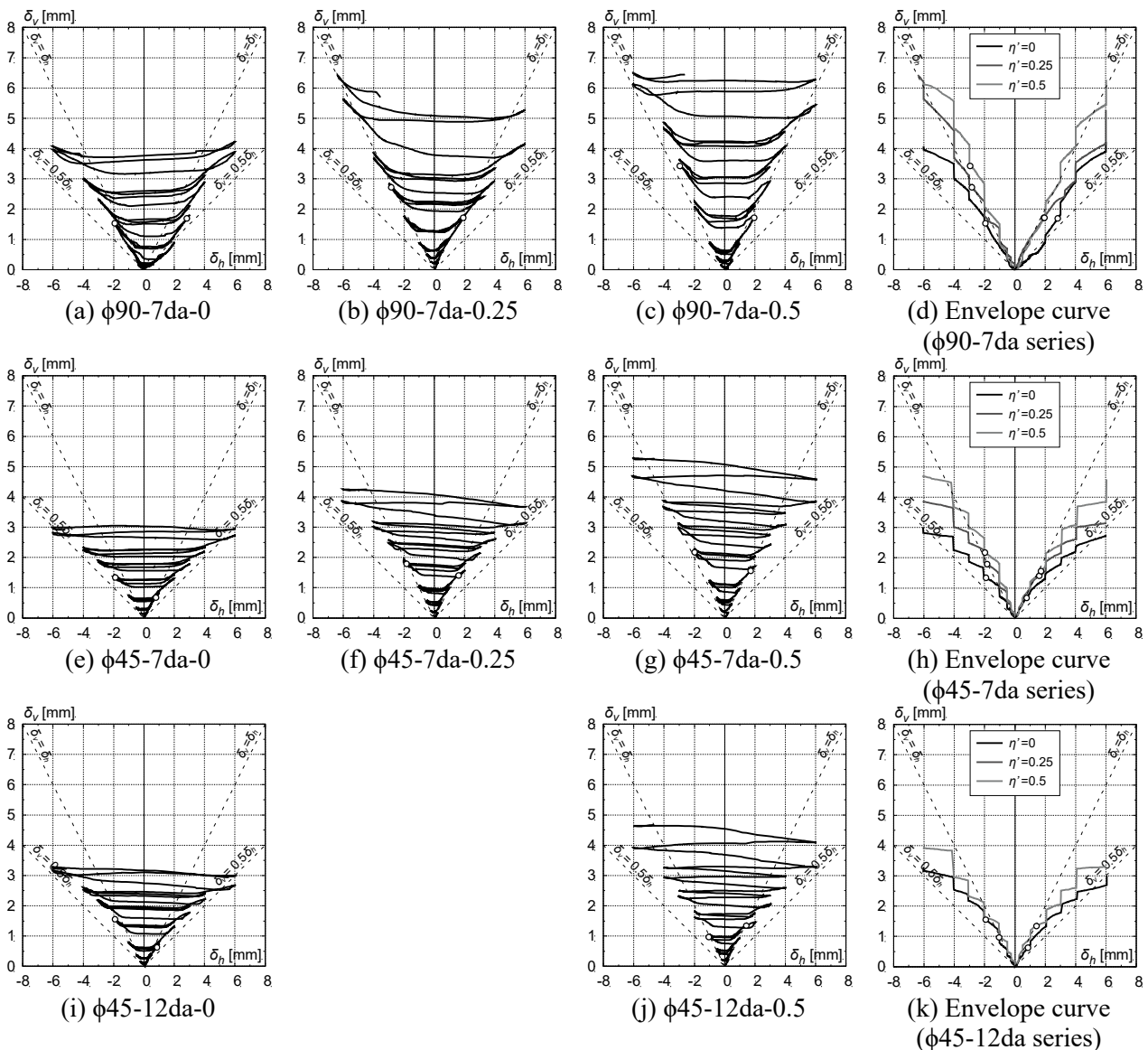


Fig. 10 – Relative vertical displacement vs. relative horizontal displacement



is smaller in $\phi 45-12da-0.5$ with embedded length $l_e=12d_a$ compared to $\phi 45-7da-0.5$ with $l_e=7d_a$, and about 14% smaller in comparison with $\delta_v|_{Q_{exp}}$.

3.3 Curvature distribution of anchor bolt

The curvature is calculated from the strain of the strain gauge stuck to the position shown in Fig.8, and the curvature distributions at $\delta_{it}=0.25, 0.5, 1.0, 2.0\text{mm}$ and at Q_{exp} are shown in Fig.11. The curvature was calculated from the following Eq. (9).

$$\phi = (\varepsilon_L - \varepsilon_R)/d_a' \tag{9}$$

where ϕ is the curvature [μ/mm]; ε_L and ε_R are the strain of the strain gauge stuck to the anchor bolt [μ]; d_a' is the diameter of the anchor bolt (after grooving) [mm].

Moreover, the curvature when ε_L and ε_R reach the yield strain is obtained from Eq. (10), and is also shown in Fig.11.

$$\phi_y = 2\varepsilon_y/d_a' \tag{10}$$

where ϕ_y is the curvature when either one of ε_L and ε_R reaches ε_y [μ/mm]; ε_y is the yield strain of the anchor bolt [μ].

It can be seen Fig. 11 that the bending deformation of the anchor bolt is concentrated on the existing side of any specimens. The maximum curvature is at the position near $2d_a$ away from the joint surface. Here, in previous study^[6], a 3D FEM analysis of the post-installed anchor is performed, and it is shown that the curvature becomes maximum at the position near $2d_a$ away from the joint surface. Therefore, the same behavior was confirmed on the existing side for both the disk shear-key and the post-installed anchor. Focusing on the curvature value of each point, it could be inferred that the anchor bolt at $2d_a$ of the existing side has reached the yielding status because the curvature of all the specimens exceeds ϕ_y . On the other hand, at other positions, it can be seen that bending deformation occurs within the elastic range, where the curvature is smaller than ϕ_y .

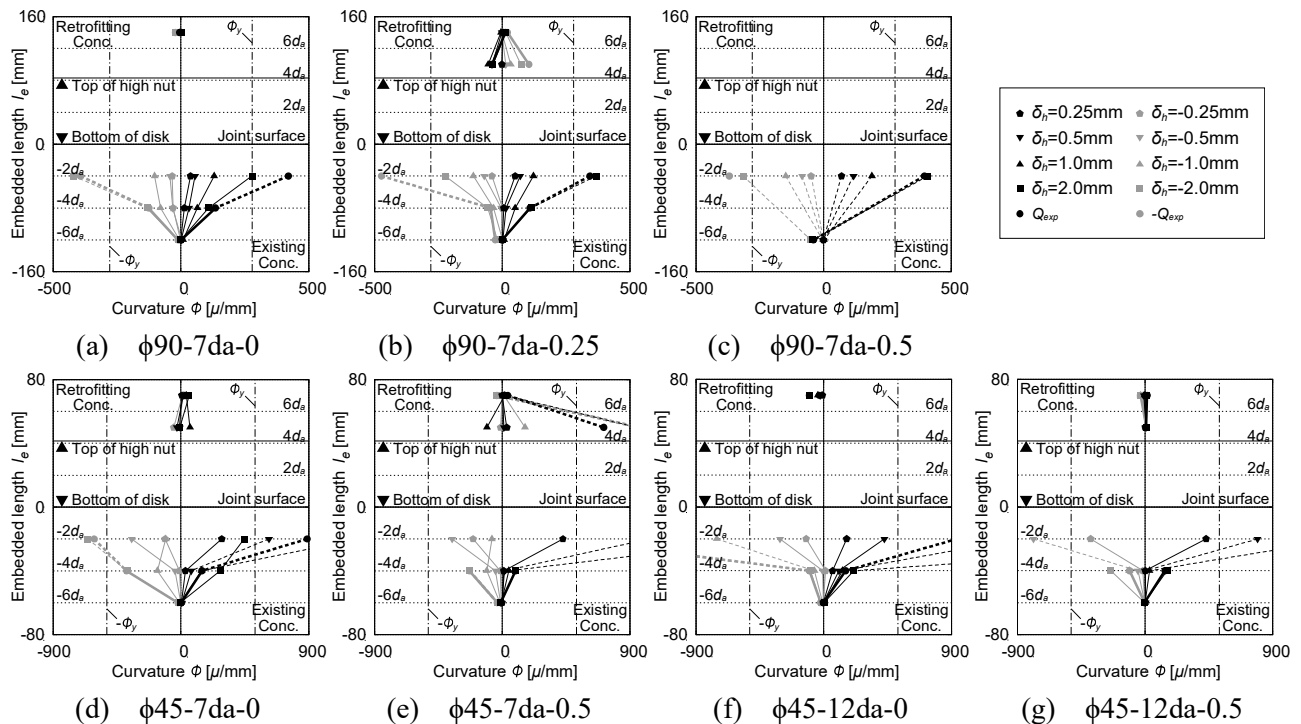


Fig. 11 – Curvature distributions of anchor bolt



4. Shear strength of disk shear-key under constant tensile force

4.1 Correspondence with current evaluation formula

The current shear strength evaluation formula of the disk shear-key is indicated in the reference [2], and the formula is shown below.

$$Q_{disk} = 0.24 \cdot K_1 \cdot K'_2 \cdot A_B \sqrt{E_c \cdot \sigma_B} \quad (11)$$

$$Q_{jd} = 0.8 \cdot Q_{disk} \quad (12)$$

$$A_B = \int_R dA_B = \int_{-\pi/4}^{\pi/4} h_d \cdot \frac{R_d}{2} d\theta = \frac{\pi \cdot R_d \cdot h_d}{4} \quad (13)$$

where Q_{disk} is the ultimate shear strength of the disk shear-key [N]; Q_{jd} is the design shear strength of the disk shear-key [N]; A_B is the effective contact area for obtaining bearing stress [mm²]; h_d is the embedded length of steel disk [mm]; K_1 is the correction coefficient by edge; K'_2 is the correction coefficient by embedded length of anchor bolt; E_c is the Young's modulus of concrete [N/mm²]; σ_B is the compressive strength of concrete [N/mm²]. In this experiment, $K_1=K'_2=1.0$ for all the specimens.

The relationship between the shear strength Q_{exp} of the all specimens in this experiment and the ultimate shear strength Q_{disk} according to Eq. (11) is shown in Fig.12. The results of element experiments of the disk shear-key^{[1],[2],[7]} that were conducted in the past are also shown in Fig.12. As shown in Section 3.1, the lower limit value of the results of previous element experiments can be evaluated with the current evaluation formula of $0.8Q_{disk}$, so the design shear strength Q_{jd} is to be obtained by Eq. (12). However, in this experiment, the maximum shear strength Q_{exp} is smaller than the ultimate shear strength Q_{disk} in all specimens. Furthermore, even in the case of tensile force ratio $\eta'=0$, it is just nearly equal to the design shear strength Q_{jd} . As the reason for that, since this experiment assumes application to external seismic retrofitting, loading control is carried out so that stress does not occur in the joint surface, and the vertical load is different from the previous experiments. That is, the loading conditions are supposed to be different.

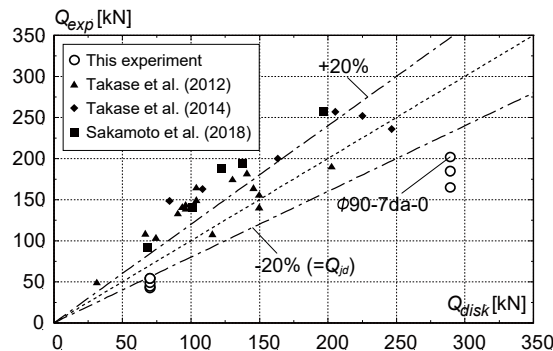


Fig. 12 – Correspondence with current evaluation formula^[2]

4.2 Evaluation method of shear strength under constant tensile force

The factors that reduce the shear strength of disk shear-key under combined stress of shear force and tensile force are considered to be the slipping out of the steel disk and the reduction of restraint effect by anchor bolt due to the tensile force. Therefore, the shear strength of disk shear-key under a constant tensile force is evaluated considering above factors based on the current evaluation formula.

First, the amount of the steel disk slipping out δ_{dv} is evaluated as the relative vertical displacement δ_v at the shear strength Q_{exp} . In this study, δ_{dv} was evaluated as an average value on each scale, and was set to 1.72mm for the $\phi 90$ series and 1.13mm for the $\phi 45$ series. Here, $\phi 90-7da-0$ was excluded. The effective contact area A_B' for obtaining the bearing stress considered δ_{dv} is calculated by Eq. (14) based on the Eq. (13).



$$A_B' = \int_{-\pi/4}^{\pi/4} (h_d - \delta_{dv}) \cdot \frac{R_d}{2} d\theta = \frac{\pi \cdot R_d \cdot (h_d - \delta_{dv})}{4} \quad (14)$$

Next, the reduction of restraint effect by anchor bolt due to the tensile force is considered using the ultimate strength of the anchor bolt subjected to the combined load of tensile force and shear force. The ultimate strength of the anchor bolt subjected to the combined load can be calculated by Eq. (15) according to reference [5]. In addition, reduction coefficient K_T of restraint effect by anchor bolt due to the tensile force is the shear strength of the anchor bolt Q_a divided by the shear strength of the anchor bolt when tensile force is not applied Q_{ay} . Here, α is proposed to be 1.0~1.5 in reference [8]. Therefore, the intermediate value $\alpha=1.25$ is used in this study.

$$\left\{ \frac{p}{p_u} \right\}^\alpha + \left\{ \frac{q}{q_u} \right\}^\alpha = \left\{ \frac{T_\eta}{T_{min}} \right\}^\alpha + \left\{ \frac{Q_a}{Q_{ay}} \right\}^\alpha = \{\eta'\}^\alpha + \{K_T\}^\alpha = 1 \quad (15)$$

where p is the tensile strength ($=T_\eta$); q is the shear strength ($=Q_a$); p_u is the tensile strength when shear force is not applied; q_u is the shear strength when tensile force is not applied.

Further, K_T can be calculated using the tensile force ratio η' from Eq. (15) as shown below.

$$K_T = \frac{Q_a}{Q_{ay}} = \sqrt[\alpha]{1 - \eta'^\alpha} \quad (16)$$

The modified shear strength evaluation formula is shown below.

$$Q'_{disk} = 0.24 \cdot K_1 \cdot K'_2 \cdot K_T \cdot A_B' \sqrt{E_C \cdot \sigma_B} \quad (17)$$

The relationship between the shear strength Q_{exp} of the all specimens in this experiment and the shear strength Q_{disk} according to Eq. (17) is shown in Fig.13. It can be confirmed that the shear strength Q_{exp} of the experimental results can be approximately evaluated by the modified evaluation formula.

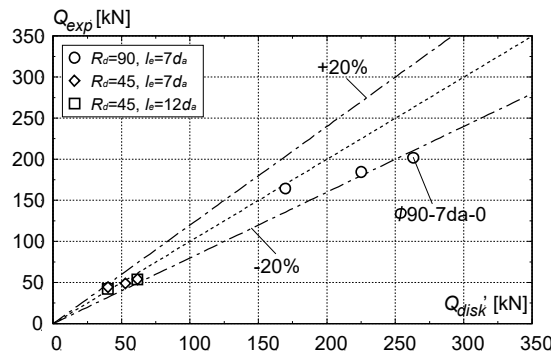


Fig. 13 – Correspondence with modified evaluation formula

5. Conclusion

In this study, the element experiments of the disk shear-key under combined stress were conducted using the steel disk diameter, the embedded length and the tensile force ratio as parameters. From the results, the following knowledges were obtained.

- (1) The shear strength of the specimens in this experiment was less than the ultimate shear strength according to the current evaluation formula. As this reason, in the previous experiment^[2] that is the basis of the current evaluation formula, the relative vertical displacement of the joint surface is controlled to be 1/2 of the relative horizontal displacement ($\delta_v=1/2\delta_h$) on the assumption of application to internal seismic retrofitting. This is considered to be caused by the different loading condition in the vertical direction between the two experiments. However, when the vertical stress generated at the joint surface is zero



($\eta'=0$), the shear strength of the disk shear-key can be roughly estimated by the design shear strength according to the current evaluation formula.

- (2) When the tensile force is not applied ($\eta'=0$), the relative vertical displacement is larger than the previous experiment^[2]. Also, the relative vertical displacement tends to increase as the tensile force increases. In other words, when applying a disk shear-key to the external seismic reinforcement, it is suggested that the steel disk slips out, and it is believed that the shear resistance decreases due to the strength reduction in the bearing stress area of the concrete.
- (3) The curvature of the anchor bolt is maximized at the position near $2d_a$ away from the joint surface on the existing side, and the value reaches the yielding region. However, curvatures within the elastic range occur at the other measurement points, and bending deformation hardly occurs at the retrofitting part. In addition, as the tensile force increases, the curvature also increases.
- (4) When cyclic shear force is applied, the shear strength of the joint decreases as the tensile force is applied. However, the relative horizontal displacement at maximum shear strength is 2mm or less, which is the allowable value of the horizontal displacement of the external seismic retrofitting joint^[4].
- (5) The factors that reduce the shear strength of the disk shear-key under combined stress of shear force and tensile force are considered to be the slipping out of the steel disk and the reduction of restraint effect by anchor bolt due to the tensile force. Therefore, the evaluation formula was modified in consideration of those factors. As a result, the shear strength was approximately evaluated.

6. Acknowledgements

This work was supported by JST Program on Open Innovation Platform with Enterprises (JPMJOP1723), Research Institute and Academia.

7. References

- [1] Takase Y et al. (2012): Basic Investigation of New Joint Element Having High Shear Strength and Stiffness for Earthquake Retrofitting of Concrete Structures, Study on Shear-key Consisted of Steel Disk and Anchor Bolt for Earthquake Retrofitting. *Journal of Structural and Construction Engineering (Transactions of AIJ)*, **77** (681), 1727-1736. (in Japanese)
- [2] Takase Y et al. (2014): Estimation Method of Horizontal Capacity of Joint Fracture for Retrofitted Frame Using Disk Shear-key, Study on Shear-key Consisted of Steel Disk and Anchor Bolt for Seismic Retrofitting. *Journal of Structural and Construction Engineering (Transactions of AIJ)*, **79** (698), 507-515. (in Japanese)
- [3] Takase Y et al. (2015): Adaptability of Disk Shear-key to Joint of Expanded Slab and Estimation of Horizontal Capacity, Study on Shear-key Consisted of Steel Disk and Anchor Bolt for Seismic Retrofitting. *Journal of Structural and Construction Engineering (Transactions of AIJ)*, **80** (708), 297-307. (in Japanese)
- [4] Japan Building Disaster Prevention Association (2002): *External Seismic Retrofitting Manual for Existing Reinforced Concrete Buildings*. (in Japanese)
- [5] Architectural Institute of Japan (2010): *Design Recommendations for Composite Constructions*. (in Japanese)
- [6] Ishida Y et al. (2018): 3D FEM Analysis of Post-installed Adhesive Anchors under Combined Stress, Stress Transmission Mechanism and Mechanical Behavior of the Joints for External Seismic Retrofitting Part 1. *Journal of Structural and Construction Engineering (Transactions of AIJ)*, **83** (751), 1307-1317. (in Japanese)
- [7] Sakamoto K et al. (2018): Development of Joint Member Using Steel Disk and Anchor Bolt for Seismic Retrofit, Part.22 Evaluation of Shear Strength of Indirect Joints Repaired by Concrete Surface Roughening and PCM. *Summaries of Technical Papers of Annual Meeting, Structures-IV*, 131-132, Architectural Institute of Japan, Sendai, Japan. (in Japanese)
- [8] Takase T et al. (2017): Mechanical Behaviour and Work of Adhesive Post-installed Anchors Subjected to Cyclic Shear Force and Constant Tensile Force. *Journal of Structural and Construction Engineering (Transactions of AIJ)*, **82** (738), 1255-1263. (in Japanese)